# Ion Beam Induced Formation and Interrogation of Au Nanoclusters

P. Karmakar,[1] G. F. Liu,[1] Z. Sroubek,[1,2] and J. A. Yarmoff[1,*]

[1]*Department of Physics and Astronomy, University of California, Riverside, California 92521, USA*

[2]*Institute of Photonics and Electronics, Czech Academy of Sciences, Chaberská 57, 182 51, Prague 8, Czech Republic*

(Received 20 March 2007; published 24 May 2007)

Low-energy ion bombardment of a Au thin film by 0.5 keV $Ar^+$ forms self-organized nanoclusters that display quantum size effects. The reduction of Au coverage with sputtering time is quantified with x-ray photoemission spectroscopy, and a decrease of both the rms roughness and correlation length is measured by STM. Neutralization of scattered 3 keV $Na^+$ and $K^+$ alkali-metal ions is used to probe the electronic states of the sputter-induced nanoclusters. The neutral fractions gradually increase as the cluster dimensions decrease, indicating that the electronic structure is similar to that of clusters grown by deposition.

DOI: 10.1103/PhysRevLett.98.215502 PACS numbers: 61.80.Jh, 68.49.Sf, 68.55.−a, 73.22.−f

Nanostructured materials have opened possibilities for new technology and basic science research in areas ranging from microelectronics to catalysis. Changes in electronic structure that scale with the cluster dimensions, i.e., quantum size effects, can strongly contribute to the chemical, electrical, and optical properties of the materials [1,2]. A formidable effort is therefore underway to develop experimental techniques that are able to produce nanostructures in a controlled manner, as well as to measure their electronic properties. Here, low-energy ion beams are shown to be promising candidates for both the fabrication and characterization of nanoclusters.

It has been reported that the interplay between sputtering and surface diffusion during ion bombardment produces well-defined nanostructures of semiconductor and metal materials [3–7]. Such a process can lead to a low-cost, large-scale method of nanomaterial production. By adjusting the ion beam parameters, such as kinetic energy, ion fluence, and projectile-target geometry, the size and shape of the nanostructures can be controlled. There has been much previous work investigating ripple and dot formation on semiconductor materials, such as Si, GaSb, and InP [3–5], but there has been relatively little work on metals [8,9]. In particular, metal clusters on transition metal oxide surfaces have not been produced by direct ion bombardment. In addition, most of the work done on sputtering-induced nanostructure formation was limited to investigations of their morphological evolution, rather than their electronic properties.

The characterization of the electronic properties of nanostructures requires a technique that can probe electronic states while distinguishing between the nanocluster and the support. The neutralization of scattered low-energy alkali-metal ions is a function of the target Fermi energy position, localized surface states [10,11] and the local electrostatic potential at the scattering site [12]. The energy of the scattered projectile can be used to separate the signal from the nanocluster from that of the support. This technique has recently been able to detect the confined states of vapor deposited Au [13,14] and Ag [15] nanoclusters.

In this Letter, we demonstrate for the first time that low-energy ion beams enable simple, but efficient methods for the controlled production and characterization of nanostructures that exhibit quantum size effects. Low-exnergy $Ar^+$ beams are used to produce and control the size and shape of Au nanoclusters on a $TiO_2$ substrate, while the neutralization of scattered $Na^+$ and $K^+$ ions is used to probe the electronic properties of the material.

The experiments were performed in an ultrahigh vacuum chamber with a base pressure of $1 \times 10^{-10}$ Torr. The $TiO_2(110)$ single crystal substrate was attached to a Ta holder, and loaded onto an *XYZ* rotary manipulator. An infrared pyrometer was used to measure the sample temperature, which was calibrated by a thermocouple attached at the edge. The crystal surface was cleaned by cycles of ion bombardment and annealing (500 eV $Ar^+$ for 10 min, followed by a 10 min anneal at 975 K) until a sharp $(1 \times 1)$ low-energy electron diffraction pattern was obtained. A thin Au film ( $\sim 60$ ML) was deposited from an evaporator consisting of Au wire (99.999%, Alfa Aesar) wrapped around a *W* filament (Mathis). The deposition rate was calibrated with a quartz crystal thickness monitor that was placed precisely at the sample position.

The Au film was sputtered by normally incident 0.5 keV $Ar^+$ (current density $= 1\ \mu A/cm^2$) at various ion fluences. All depositions, sputtering and ion scattering measurements were performed with the sample at room temperature. Images of the Au clusters after each deposition and sputtering cycle were collected with an *in situ* scanning tunneling microscope (STM, Park Scientific Autoprobe VT). The images were collected in constant current mode with a tunneling current of 1 nA and a sample bias of $-1.5$ V. The surface roughness and correlation length, which are related to the vertical and lateral dimensions of the nanostructures, respectively, were quantitatively determined from the STM images. The purity and Au coverage were measured with x-ray photoelectron spectroscopy (XPS) immediately after cleaning and again following each deposition and sputtering cycle.

 

Time-of-flight was used to measure the charge state-resolved kinetic energy distributions of scattered $Na^+$ and $K^+$ ions, as described elsewhere [14]. A thermionic emitter ion gun (Kimball Physics) generated 3 keV alkali-metal ion beams, which were deflected across a 1.0 $mm^2$ aperture to produce pulses ( $\sim$ 10 ns) at a rate of 80 kHz. The beams were incident normally to the surface, and the ions and neutrals scattered at 150° were detected by a microchannelplate (MCP) array after traveling through a 0.55 m long flight tube containing a pair of deflection plates. "Total Yield" spectra were collected with the deflection plates held at ground, while "Neutrals Only" spectra were collected by placing 300 V between the plates to remove the scattered ions.

STM topography of the thin Au film is presented in Fig. 1(a). The morphology of the thick film is rough and contains large-scale features. Zhang, *et al.* studied the growth and the surface morphology of Au on $TiO_2(110)$ with high resolution scanning electron microscopy [16]. They observed that at 300 K, the Au film morphology evolves with coverage from hemispherical islands initially, to partially coalesced wormlike island structures, and finally to a continuous rough film. Similar structures also were observed for thin films grown by sputter deposition [9,17].

The surface morphology and Au coverage changes as a function of $Ar^+$ ion fluence. Figure 1(b) shows a typical STM image collected after $Ar^+$ sputtering at a fluence of $5 \times 10^{16}$ ions/$cm^2$. The rms roughness and correlation length of the features on the surface decrease with ion fluence, as shown in Fig. 2(a). Figure 2(b) presents the XPS intensity of the Au 4*f* and Ti 2*p* core levels as a function of ion fluence. It shows a decrease of the Au and an increase of the Ti signal with $Ar^+$ sputtering, which indicates that Au is removed thereby revealing the $TiO_2$ substrate. From the STM and XPS measurements, it can be concluded that both the lateral and vertical dimensions of the structures decrease as the Au is sputtered, leading to the formation of nanoscale clusters.

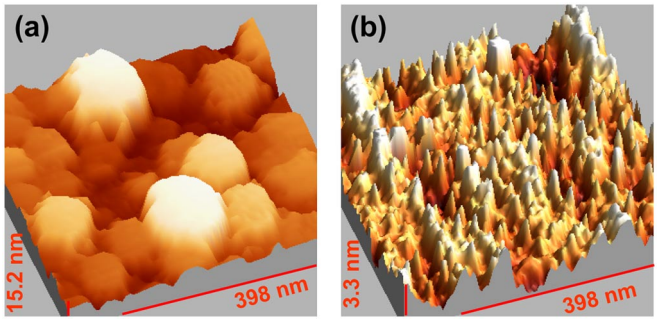


FIG. 1 (color online). 3D STM topographies of (a) a ~60 ML Au thin film deposited on $TiO_2$, and (b) after 0.5 keV $Ar^+$ ion sputtering at a fluence of $5 \times 10^{16}$ ions/ $cm^2$. The images show an area of 398 nm × 398 nm, while the *z* dimension is scaled to the size of the largest feature.

The shape and size of the Au clusters formed by deposition on $TiO_2$ depend largely on the condition of initial surface [18], while the clusters formed by sputtering depend on the ion beam parameters. Tersoff predicted that self-organized growth of nanostructures during deposition is driven by the misfit strain in heteroepitaxial systems [19]. Nanostructures formed by ion sputtering are instead produced by a temporally and spatially correlated creation of vacancies and adatoms [20]. The morphology of sputtered-induced nanoclusters can be controlled with ion beam parameters such as kinetic energy, flux, fluence, and the target geometry. Ion sputtering could also be used to reduce the dimensions of prefabricated nanostructures, such as aluminum nanowires and aluminum single electron transistors [21].

The morphology and time evolution of ion sputtered surfaces have been described by a continuum equation [5] based on Sigmund's sputtering theory [22]. The theory for amorphous or polycrystalline targets assumes that most of the energy of the incident ion is transferred at a distance (penetration depth) below the surface and distributed via collisions into a Gaussian ellipsoid with specific longitudinal and lateral widths. The probability that a surface atom is ejected is proportional to the energy transferred to that point from all atoms that participate in the collision cascade. Bradley and Harper (BH) [23] predicted that the overall amount of deposited energy, and therefore the number of emitted atoms, is sensitive to the local surface curvature. Surface atoms are sputtered preferentially from valleys, whereas emission from the top of mountains is inhibited, which leads to formation of self-organized nanostructures. Recently, a generalization of the BH linear theory has been introduced to describe other effects of

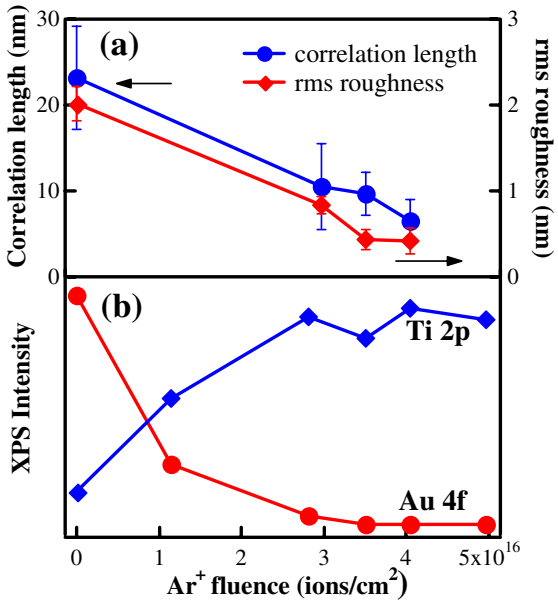


FIG. 2 (color online). (a) The correlation length and rms roughness and (b) the ratio of the Au and Ti XPS signals shown as a function of $Ar^+$ ion fluence.

ion bombardment, such as dot and hole formation and the variation of structures with ion energy or fluence [5–7].

The formation of dotlike structures by 0.5 keV $Ar^+$ sputtering on $Au/TiO_2$ is consistent with the existing theory, but the theory cannot explain the decrease of the rms roughness and correlation length with ion fluence [Fig. 2(a)]. Note, however, that Chen, *et al.* [24] bombarded Ge on Si with 300 eV $Ar^+$ and Krishna, *et al.* [25] bombarded zinc oxide films on Si(100) with 15 keV $Ar^+$, and both observed that the rms roughness and the diameter of the clusters decrease with ion fluence similar to the results reported here. Interestingly, nanodots of Si on Si [26] and Pt nanostructures on Si [27] produced by ion sputtering also decrease their dimensions with further sputtering. The existing theory predicts that the rms roughness would initially increase and saturate after a certain time $t_x$, called the crossover time. This theory fits some experimental observations well, such as when the surfaces of bulk materials or very thick films are sputtered, but it cannot explain a decrease of rms roughness during thin film or nanostructure sputtering. A possible explanation may be that the dynamic balance between growth and erosion is not same when ions bombard a nanostructure or very thin film instead of a flat, uniform surface. It may be possible to include an extra smoothing term in the continuum equation, however, to explain the decrease of rms roughness and correlation length during ion sputtering of such thin films and nanoclusters.

The electronic properties of the Au nanoclusters produced by sputtering are investigated via the neutralization of scattered low-energy $Na^+$ and $K^+$ ions. When an alkali-metal atomic particle is in the vicinity of a surface, its ionization level shifts up due to the image charge interaction, while it also broadens due to interaction of the ion and surface wave functions [28]. The neutralization probability of a scattered alkali-metal ion is determined along the outgoing trajectory by a nonadiabatic resonant charge transfer process, typically within about 5 a.u. of the surface. The measured neutral fraction (NF) depends on the ionization potential, the degree that the level shifts near the surface, and the local electrostatic potential at the point where the charge state distribution is frozen in.

Figure 3 shows the neutral fractions of scattered $Na^+$ and $K^+$ ions as a function of $Ar^+$ ion fluence. The NF for $Na^+$ scattered from the thick Au film is ~3% which is the expected value for scattering from bulk Au [13]. As the $Ar^+$ bombardment produces nanoclusters and reduces their dimensions, the NF increases and eventually reaches a value of ~48%. Similarly large values of the NF for scattered $Na^+$ were obtained previously from the smallest Au clusters formed by vapor deposition onto $TiO_2(110)$ [13]. Figure 3 also shows the same measurement with $K^+$ ions, where in this case the NF for the Au film is zero, and gradually increases to 20% with $Ar^+$ sputtering.

It should be pointed out that changes in the roughness of the Au film with sputtering could possibly contribute to the alkali-metal ion scattering NF changes. To study the effects

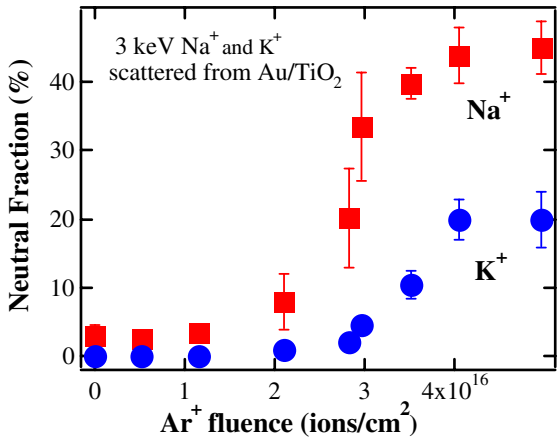


FIG. 3 (color online). Neutral fractions of 3 keV $Na^+$ and $K^+$ ions singly scattered from a sputtered Au film shown as a function of the $Ar^+$ ion fluence.

of roughness, a clean polycrystalline Au foil was sputtered with $Ar^+$ under the same experimental conditions used for sputtering the Au film on $TiO_2$, but no concurrent changes in the scattered alkali-metal ion neutralization were observed. It was also previously observed that $Ar^+$ sputtering of a Au foil [13] and Au(111) [15] does not change the surface work function or increase the neutralization during alkali-metal ion scattering. Therefore, the increase of NF with sputtering of Au clusters on $TiO_2$ cannot be explained simply by a change of surface roughness.

In addition, it is possible that the projected band gap and surface states that exist in noble metal (111) surfaces could influence the measured neutral fractions [10]. The production of Au (111) facets by vapor deposition at room temperature is not impossible, but they would be deformed in the early stages of ion bombardment before the nanoclusters are produced. Since changes of the NF during the early stages of ion bombardment were never seen, it can be concluded that any contribution of (111) surface states to the NF can be neglected.

The increase of both the Na and K NF's with sputtering can be explained by the size-dependent electronic structure of the nanoparticles. As the Au film is sputtered, the morphology of the surface is strongly modified and isolated Au clusters are produced. Ion sputtering decreases both the lateral and vertical dimensions of the Au clusters (see Fig. 2), so that quantum confinement is possible in either direction. In the case of sputtering, 2D confinement is more probable as the cluster's vertical dimension is smaller than the lateral dimension, as observed from STM [Fig. 2(a)]. Hövel and Brake [29] presented size-dependent $dI/dV$ curves of STS measurements of small Au clusters on graphite, and found that the peak position changes with cluster height. STS spectra of Ag clusters on alumina showed discrete electronic states along the vertical direction [30]. Accordingly, occupied or partially occupied confined states may appear and shift towards vacuum level with lowering of the cluster dimensions with $Ar^+$ sputtering. These states can contribute directly to the neutraliza-

tion of the scattered alkali-metal ion, as described previously [13].

An additional contribution to the size-dependent neutralization may be the dependence of the magnitude of the image charge potential on the cluster size. It can be shown from classical electrodynamics [31] that the image charge potential is reduced when the clusters become smaller, leading to less of an upward shift of the ionization level. At typical distances of 5 a.u. from the image plane of a flat metal surface, where charge exchange between the projectile and the substrate typically occurs, the image charge potential shift is 1.7 eV, whereas the shift induced by clusters with diameters of 20 a.u is only 0.7 eV.

Thus, there are two contributing factors that act to raise the NF as the cluster dimensions decrease with sputtering time. The appearance and upward shift of the confined states and the reduction of the image charge potential each lead to an increased overlap of the alkali-metal ionization levels with the occupied cluster states. The higher NF observed for Na than for K is understandable because the K ionization level is always positioned above the ionization level of Na.

It should be mentioned that presence of the support material could influence the characteristics of the Au nanoclusters. The NF does not increase when a bulk Au foil is sputtered, even though it may form a similar surface morphology as the sputtered Au film on $TiO_2$. This suggests that isolated quantum confined systems are not produced when nanometer sized quantum dots are supported on the same material. Facsko *et al.* also observed confined states in sputtered-induced GaSb dots when they were supported on AlSb, but not on GaSb [3]. Note that there is evidence in the literature that the support material affects the catalytic properties of Au nanoclusters, which may also be related to their electronic structure [2]. Clearly, experiments with different substrates are essential in order to clarify the intrinsic nature of the confined states. The techniques of ion bombardment and ion scattering are sufficiently flexible to make such studies feasible.

In conclusion, the work reported here shows that low-energy ion sputtering produces Au nanoclusters in a controllable manner, and that these clusters exhibit electronic size effects. The combination of keV ion sputtering and alkali-metal ion scattering provides a unique method for producing and probing nanomaterials. In particular, the sensitivity of low-energy alkali-metal ion scattering to the potential and electronic density of states makes this technique suitable for studying specific features of the electronic structure of spatially confined systems.

This material is based upon work supported by, or in part by, the U. S. Army Research Laboratory and U. S. Army Research Office (Contract/Grant No. 46686-PH-H).

*Corresponding author.
Electronic address: yarmoff@ucr.edu

[1] J. P. Wilcoxon and B. L. Abrams, Chemical Society Reviews **35**, 1162 (2006).
[2] M. S. Chen and D. W. Goodman, Catal Today **111**, 22 (2006).
[3] S. Facsko, T. Dekorsy, C. Koerdt, C. Trappe, H. Kurz, A. Vogt, and H. L. Hartnagel, Science **285** 1551 (1999).
[4] F. Frost, A. Schindler, and F. Bigl, Phys. Rev. Lett. **85**, 4116 (2000).
[5] M. A. Makeev, R. Cuerno, and A. L. Barabasi, Nucl. Instrum. Methods Phys. Res., Sect. B **197**, 185 (2002).
[6] B. Kahng, H. Jeong, and A. L. Barabasi, Appl. Phys. Lett. **78**, 805 (2001).
[7] M. Castro, R. Cuerno, L. Vázquez, and R. Gago, Phys. Rev. Lett. **94**, 016102 (2005).
[8] U. Valbusa, C. Boragno, and F. Buatier de Mongeot, J. Phys. Condens. Matter **14**, 8153 (2002).
[9] P. Karmakar and D. Ghose, Surf. Sci. **554**, L101 (2004).
[10] A. R. Canario, T. Kravchuk, and V. A. Esaulov, New J. Phys. **8**, 227 (2006).
[11] Y. Yang and J. A. Yarmoff, Phys. Rev. Lett. **89**, 196102 (2002).
[12] J. A. Yarmoff, Y. Yang, and Z. Sroubek, Phys. Rev. Lett. **91**, 086104 (2003).
[13] G. F. Liu, Z. Sroubek, and J. A. Yarmoff, Phys. Rev. Lett. **92**, 216801 (2004).
[14] G. F. Liu, Z. Sroubek, P. Karmakar, and J. A. Yarmoff, J. Chem. Phys. **125**, 054715 (2006).
[15] A. R. Canario and V. A. Esaulov, J. Chem. Phys. **124**, 224710 (2006).
[16] L. Zhang, F. Cosandey, R. Persaud, and T. E. Madey, Surf. Sci. **439**, 73 (1999).
[17] G. S. Bales, R. Bruinsma, E. A. Eklund, R. P. U. Karunasiri, J. Rudnick, and A. Zangwill, Science **249**, 264 (1990).
[18] S. C. Parker, A. W. Grant, V. A. Bondzie, and C. T. Campbell, Surf. Sci. **441**, 10 (1999).
[19] J. Tersoff, Physica (Amsterdam) **E3**, 89 (1998).
[20] G. Costantini, F. Buatier de Mongeot, C. Boragno, and U. Valbusa, Phys. Rev. Lett. **86**, 838 (2001).
[21] M. Savolainen, V. Touboltsev, P. Koppinen, K.-P. Riikonen, and K. Arutyunov, Appl. Phys. A **79**, 1769 (2004).
[22] P. Sigmund, Phys. Rev. **184**, 383 (1969).
[23] R. M. Bradley and J. M. E. Harper, J. Vac. Sci. Technol. A **6**, 2390 (1988).
[24] H. C. Chen, C. M. Huang, K. F. Liao, S. W. Lee, C. H. Hsu, and L. J. Chen, Nucl. Instrum. Methods Phys. Res., Sect. B **237**, 465 (2005).
[25] R. Krishna, V. Baranwal, Y. S. Katharria, D. Kabiraj, A. Tripathi, F. Singh, S. A. Khan, A. C. Panday, and D. Kanjilal, Nucl. Instrum. Methods Phys. Res., Sect. B **244**, 78 (2006).
[26] W. B. Fan, L. J. Qi, H. T. Sun, Y. Y. Zhao, and M. Lu, Nanotechnology **17**, 1878 (2006).
[27] P. Karmakar and D. Ghose, Nucl. Instrum. Methods Phys. Res., Sect. B **222**, 477 (2004).
[28] J. Los and J. J. C. Geerlings, Phys. Rep. **190**, 133 (1990).
[29] H. Hövel and I. Barke, Prog. Surf. Sci. **81**, 53 (2006).
[30] N. Nilius, M. Kulawik, H. P. Rust, and H. J. Freund, Surf. Sci. **572**, 347 (2004).
[31] L. D. Landau and E. M. Lifshitz, *Electrodynamics of Continuous Media* (Pergamon, New York, 1960).